First Principle Calculations of the Electronic and Vibrational Properties of the 3-(1,1-Dicyanoethenyl)-1-phenyl-4,5-dihydro-1H-pyrazole Molecule

ARTICLE *in* THE JOURNAL OF PHYSICAL CHEMISTRY A · FEBRUARY 2015

Impact Factor: 2.69 · DOI: 10.1021/jp510102q · Source: PubMed

5 AUTHORS, INCLUDING:

Malgorzata Makowska-Janusik
Akademia Jana Dlugosza w Czestochowie
104 PUBLICATIONS **942** CITATIONS
SEE PROFILE

Francois Kajzar
Polytechnic University of Bucharest
379 PUBLICATIONS **4,544** CITATIONS
SEE PROFILE

Andrzej Miniewicz
Wroclaw University of Technology
9 PUBLICATIONS **6** CITATIONS
SEE PROFILE

Ileana Rau
Polytechnic University of Bucharest
154 PUBLICATIONS **850** CITATIONS
SEE PROFILE

THE JOURNAL OF PHYSICAL CHEMISTRY A

Article

pubs.acs.org/JPCA

First Principle Calculations of the Electronic and Vibrational Properties of the 3-(1,1-Dicyanoethenyl)-1-phenyl-4,5-dihydro-1H-pyrazole Molecule

Malgorzata Makowska-Janusik,*[,†] Francois Kajzar,[‡,§] Andrzej Miniewicz,[∥] Lucia Mydlova,[†] and Ileana Rau[‡]

[†]Institute of Physics, Jan Dlugosz University, Al. Armii Krajowei 13/15, 42-200 Czestochowa, Poland

[‡]Faculty of Applied Chemistry and Materials Science, University Politehnica of Bucharest, Bucharest, Romania

[§]Laboratoire de Chimie, CNRS, Université Claude Bernard, ENS-Lyon, 46 Allée d'Italie, 69364 Lyon Cedex 07, France

[∥]Advanced Materials Engineering and Modelling Group, Faculty of Chemistry, Wroclaw University of Technology, Wybrzeze Wyspianskiego 27, 50-370 Wroclaw, Poland

ABSTRACT: Results of first principle quantum chemical calculations of electronic and vibrational properties of the push−pull 3-(1,1-dicyanoethenyl)-1-phenyl-4,5-dihydro-1H-pyrazole (DCNP) molecule are reported and discussed. The structure of DCNP was optimized with HF/6-311G methodology and found to be planar. On the basis of obtained geometry, infrared absorption and Raman spectra were computed within the HF/6-311++G** formalism. They allow to conclude that the changes of molecule dipole moment and variation of its polarizability appear at the same vibrational mode and affect the optical properties of the DCNP. Four different methodologies: time-dependent HF and time-dependent DFT method with B3LYP, LC-BLYP, and CAM-B3LYP potentials were used to compute the optical absorption spectra of DCNP. Influence of solvent on molecular electronic structure was studied within the C-PCM model. It predicts the DFT/B3LYP methodology as the best one to compute the NLO properties of the DCNP. The computed HOMO and LUMO orbitals show evidence that the ground state of the molecule is located at its aromatic part. The discussion of charge transfer during the excitation process for the transition S_0-S_1 was performed. The charge transfer parameter calculated in vacuum and in solvent gives the evidence that the solvent environment weakly enhance the molecular charge transfer. It confirms the tendency of an occurrence of the intermolecular charge transfer in DCNP which is crucial for its hyperpolarizability magnitude. It was proved that the second-order susceptibility corresponding to SHG may be calculated for host−guest polymer/DCNP composite using the simple oriented gas model and the rigorous local field approach should not necessarily be applied.

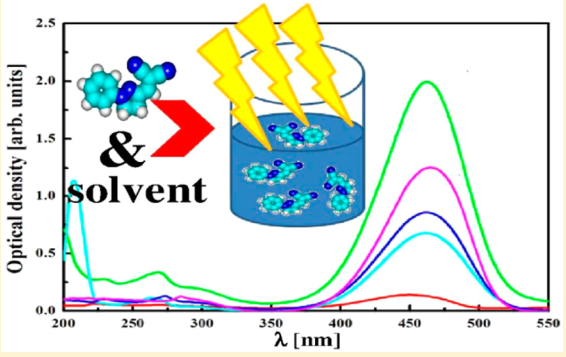

1. INTRODUCTION

The 3-(1,1-dicyanoethenyl)-1-phenyl-4,5-dihydro-1H-pyrazole (DCNP) molecule is the building block of the noncentrosymmetric organic crystal.[1] It exhibits very interesting physicochemical properties. In particular, Miniewicz et al.[2] have reported that DCNP nanocrystals show an important photoluminescence and ability to double the frequency of incoming light. One and two photon excited fluorescence in DCNP solutions were also investigated.[3] The amplified spontaneous emission (ASE) originating in DCNP embedded into poly(methyl methacrylate) (PMMA) thin films[4] as well as in other synthetic polymers and deoxyribonucleic acid (DNA) biopolymer matrices[5] was found.

The DCNP compound crystallizes in the monoclinic *Cc* space group[6] and a special, noncentrosymmetric arrangement creates the material with large linear electro-optical response (the Pockels effect), whose diagonal Pockels tensor component r_{333} is equal to 8.7×10^{-11} m/V at 632.8 nm.[7] The works by Miniewicz et al.,[8] Allen et al.,[7] and Black et al.[1] have revealed that DCNP exhibits an exceptional nonlinear optical (NLO) potential, giving the powder optical second harmonic generation (SHG) signal of approximately 100 times larger than urea when the light with wavelength of 1.9 μm is applied. Using the electric field induced second harmonic generation (EFISH) technique at 1.17 μm excitation wavelength, Allen et al.[7] measured large main molecular first hyperpolarizability $\beta(-2\omega;\omega,\omega) = 777.9 \times 10^{-30}$ esu ($\mu\beta(1.17\ \mu\text{m}) = 5445.3 \times 10^{-48}$ esu, where μ is the ground state molecular dipole moment). Its static value β_0 (0;0,0) is equal to 44.7×10^{-30} esu ($\mu\beta_0 = 312.9 \times 10^{-48}$ esu). Very recently Manea et al.[9] using the optical second harmonic generation (SHG) technique performed at the fundamental wavelength 1.064 μm obtained a

Received: October 6, 2014
Revised: January 29, 2015
Published: February 4, 2015

DOI: 10.1021/jp510102q
J. Phys. Chem. A 2015, 119, 1347−1358

large value for the diagonal quadratic susceptibility tensor component $\chi^{(2)}_{ZZZ}$ $(-2\omega;\omega,\omega)$ equal to 101 ± 10 pm/V for corona poled thin film (for a review see e.g. Kajzar et al.[10] and Dalton[11]) composed by 2 wt % of DCNP embedded in PMMA matrix. Mentioned results are in contradiction with earlier SHG measurements performed on DC field poled thin films of DCNP embedded in polyetherketone (PEK), performed at the same fundamental wavelength.[12,13] The value for the diagonal quadratic susceptibility for the DCNP/PEK composite with the dopants concentration of 20 wt % was found to be equal to $\chi^{(2)}_{ZZZ}$ $(-2\omega;\omega,\omega)$ = 20.86 pm/V. It seems that the DCNP molecule is very sensitive to the environmental effect, and the crucial role is played by the multipolar interactions. In order to explain this discrepancy and to get information on the electronic structure and photophysical properties of this interesting molecule, we have studied its electronic behavior applying first-principles quantum chemical calculations.

The chemical structure of the DCNP molecule is schematically shown in Figure 1. It is a push−pull structure exhibiting

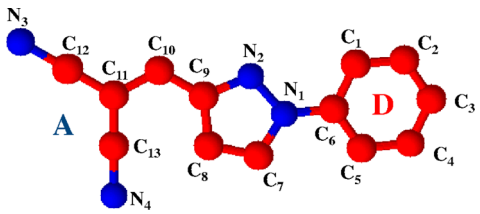

Figure 1. Scheme of the 3-(1,1-dicyanoethenyl)-1-phenyl-4,5-dihydro-1H-pyrazole (DCNP) molecule with selected donor (D) and acceptor (A) groups.

unidirectional internal charge transfer (ICT) occurring between the phenyl ring acting as electron donor and the dicyano group characterized as an acceptor. The resulting electron displacement is behind the above-mentioned large nonlinear optical (NLO) response.[3,14] The important ground state dipole moment together with the large molecular hyperpolarizability predisposes the DCNP as a chromophore embedded in amorphous polymer matrix for fabrication of NLO active guest−host materials.[10−12,15] Moreover, the DCNP crystal exhibits pyroelectric properties and produces the already mentioned very high linear electro-optic effect, owing to the very planar and layerlike solid-state packing of the compound, as deduced from the room-temperature crystal structure, determined by single-crystal X-ray diffraction.[16] The knowledge of electron transfer mechanism occurring in the molecule is also very useful to explain its electronic and optical properties. The additional view at mentioned properties may be realized by the quantum chemical calculations. To our knowledge, no such theoretical studies, including the solvent effect, have been realized. The electronic properties calculations of the DCNP as an isolated molecule were performed only by semiempirical methodology,[3] not including density functional theory or ab initio applications.

2. DETAILS OF THE QUANTUM CHEMICAL CALCULATIONS

Starting an analysis of the electronic properties of the DCNP molecule first of all its geometry was optimized applying the ab initio formalism implemented in the GAMESS program package.[17,18] The procedure was performed for an isolated molecule in vacuum. The initial geometry was built up using the ACD/ChemSketch, an integrated software package from Advanced Chemistry Development, Inc. The minimum of the potential energy surface was calculated at the restricted Hartree−Fock (RHF) level[19] with the 6-311G basis set in C_1 symmetry. The quadratic approximation (QA) optimization algorithm[20] based on augmented Hessian techniques was used to reach the geometry of the DCNP molecule possessing the minimum of the total energy. The gradient convergence tolerance was equal to 10^{-4} Hartree/Bohr. At the end of the geometry search, the Hessian evaluation was performed to exclude the structures giving negative modes and ensure the thermodynamic equilibrium of the molecule.

To predict electronic and optical properties of the DCNP molecule, the quantum chemical calculations were performed using the structure with optimized geometry. First of all the investigated molecule has been rotated in order to obtain the geometry for which its dipole moment was oriented along the Z axis. The electronic properties were computed for the isolated molecule as well as taking into account the solvent effect. The calculations were carried out applying HF methodology and density functional theory (DFT) using the GAMESS program package.[17,18] The time-dependent DFT (TDDFT) formalism is considered to be the most prominent method to calculate the excited state of medium-size and large molecules. The TDDFT calculations were performed using different exchange-correlation (XC) potentials in generalized gradient approximation (GGA), namely the B3LYP,[21−23] LC-BLYP,[24] and CAM-B3LYP[25] potentials. The single-point calculations were performed with the 6-311G basis set augmented by polarization and diffusion functions (6-311++G**).[26−28] The RHF SCF energy convergence criterion was chosen to be 10^{-12} Hartree. The UV−vis absorption spectra were calculated using the iterative Davidson method[29] with an accuracy of 10^{-12} Hartree.

In order to investigate the solvent effect on the electronic properties of DCNP, the polarizable continuum model (PCM)[30] was used, applying the conductor-like PCM (C-PCM)[31,32] implementation. It is one of the most frequently used apparent surface charge (ASC) model.[33,34] The solvent

Table 1. Dielectric Constants at Zero and Infinite Frequency of Used Solvents and the Static Dipole Moment of DCNP Molecule Calculated by Different Methods in Vacuum and in Solvent

	dielectric constant		μ (D)			
solvent	ε	ε_∞	HF	B3LYP	LC-BLYP	CAM-B3LYP
vacuum	1.00	1.00	8.35	8.74	8.26	8.43
acetonitrile	35.69	1.81	11.33 (35.69%)	12.22 (39.82%)	11.32 (37.05%)	11.58 (37.37%)
cyclohexane	2.03	2.02	9.56 (14.49%)	10.15 (16.13%)	9.50 (15.01%)	9.71 (15.18%)
methanol	32.63	1.76	11.07 (32.57%)	11.95 (36.73%)	11.07 (34.02%)	11.34 (34.52%)
tetrahydrofuran	7.58	1.97	10.70 (28.14%)	11.50 (31.58%)	10.68 (29.30%)	10.94 (29.77%)
toluene	2.38	2.23	9.77 (17.01%)	10.39 (18.88%0	9.72 (17.68%)	9.94 (17.91%)

DOI: 10.1021/jp510102q
J. Phys. Chem. A 2015, 119, 1347−1358

radii and the dielectric constants were defined the same as the parameters collected in GAMESS code. The implemented dielectric constant values of investigated solvents are specified in Table 1.

3. RESULTS AND DISCUSSION

3.1. Geometry of the DCNP Molecule. As already mentioned, before starting the essential calculations, the geometry of the DCNP molecule was optimized using the HF/6-311G methodology. The obtained interatomic distances and other structural parameters are collected in Table 2. Also

Table 2. Computed Bond Lengths as Well-Selected Dihedrals and Torsion Angles Obtained Using the Geometry Optimization Done by the HF/6-31G Methodology[a]

length of bonds (Å)					
bond	calcd values	exptl data	bond	calcd values	experimental data
C_1-C_2	1.382	1.391	C_7-C_8	1.542	1.543
C_2-C_3	1.389	1.399	C_8-C_9	1.516	1.522
C_3-C_4	1.383	1.385	C_9-C_{10}	1.442	1.420
C_4-C_5	1.388	1.408	$C_{10}-C_{11}$	1.344	1.364
C_5-C_6	1.392	1.411	$C_{11}-C_{12}$	1.431	1.439
C_6-C_1	1.395	1.395	$C_{11}-C_{13}$	1.434	1.446
N_1-C_6	1.398	1.404	N_3-C_{12}	1.142	1.156
N_1-C_7	1.470	1.493	N_4-C_{13}	1.141	1.144
N_2-C_9	1.280	1.317	N_1-N_2	1.340	1.333
torsion angles (deg)		calculated data	dihedral angles (deg)		calculated data
$N_2-N_1-C_7-C_6$		179.998	$C_{11}-C_{10}-C_9-C_8$		179.960
$N_2-C_9-C_8-C_{10}$		179.991	$N_2-N_1-C_6-C_1$		179.956
$C_{12}-C_{11}-C_{13}-C_{10}$		179.994	$C_{13}-C_{11}-C_{10}-C_9$		0.008

[a]Experimental bond lengths are from ref 16.

the DFT methodology was used to optimize the structure of the DCNP molecule, but the obtained results were unsatisfactory. It is known that the DFT/GGA and hybrid functionals tend to overestimate the length of interatomic distances.[35,36]

Analyzing data appearing in Table 2, one may see that the investigated molecule is flat. It is confirmed by the specified dihedral and torsion angles. The fact that the geometry of the molecule is correct can be concluded, *inter alia*, on the basis of qualitative analysis of the interatomic bond lengths. The shortest bonds are the triple ones, namely $N_3{\equiv}C_{12}$ and $N_4{\equiv}C_{13}$ (see Figure 1). The double bond $N_2{=}C_9$ has length 1.280 Å, and the length of bond $C_{10}-C_{11}$ is equal to 1.344 Å. The bonds in the phenyl ring are slightly longer. A comparison of the calculated bond lengths with the experimentally measured ones show a good agreement between them, as seen from Table 1. It confirms that the HF/6-311G methodology may be used to reproduce the geometry of the DCNP molecule. As a consequence, the proposed quantum chemical method is appropriate to calculate the vibrational properties of the investigated molecular structure.

3.2. IR and Raman Spectra. The stability of the investigated structure was studied by calculation of infrared (IR) and Raman spectra, presented in Figure 2. The mentioned spectra were calculated at the HF/6-311G methodology in vacuum and scaled by the factor 0.90. It is in accordance with the work of Scott and Radom[37] who recommended the use of a

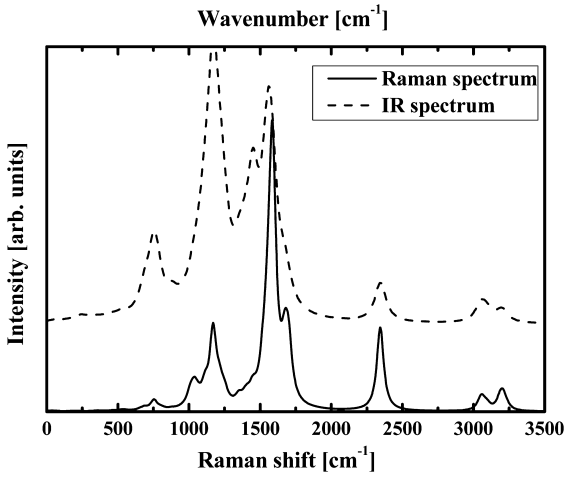

Figure 2. IR absorption and Raman spectra calculated for the DCNP molecule in vacuum using HF/6-311G methodology.

scale factor of 0.9054 for the vibrational frequencies calculated at HF/6-31++g(d,p). The IR and Raman spectra of DCNP closely resemble each other and by analyzing them one can see that some of the main bands show similar wavenumbers and relative intensities. The bands at 754.4 cm^{-1}, 1169.9 cm^{-1}, 1561.9 cm^{-1}, 2345.3 cm^{-1}, 3059.0 cm^{-1}, and 3182.0 cm^{-1} in IR absorption spectrum are correlated with those in the Raman spectrum. These bands must be associated with specific modes that are simultaneously strongly active both in IR and in Raman spectra. This phenomenon is quite unusual even in the absence of an inversion symmetry. The existence of IR and Raman activity at the same vibration means that at the same time the molecular dipole moment and the polarizability of the molecule change. Mentioned behavior may be observed for specific push−pull molecules, where instead the existence of one-directional charge transfer from donor to acceptor through the single−double conjugated bond path additional direction of charge carrier transfer is observed.[38] Mentioned mechanism induces large variation of both the molecular dipole moment and of the molecular polarizability, during the same vibration. Analyzing the IR and Raman spectra presented in Figure 2, one can see that both behave complementary: the strongest bands in IR spectrum are weak in the Raman spectrum and vice versa. Additionally, in the Raman spectrum are present peaks at 1038.5 and 1674.1 cm^{-1}, which are absent in the IR absorption spectrum. On the contrary, in the IR spectrum, one can observe the peak at 1453.5 cm^{-1} not observed in the Raman spectrum. The presented spectra are generally very broad starting, from 500 cm^{-1} up to 1600 cm^{-1}, what is typical for compounds with strong hydrogen bonds.

The frequencies of Raman shifts calculated for isolated (in vacuum) DCNP molecule in its electronic ground state were compared to the experimentally measured Raman spectrum obtained for single crystal of DCNP at 295 K. The parameters of the performed experiment are characterized in the work of Morawski et al.[39] Comparing data collected in Table 3 (column 1 with 2), one can see that the vibrational frequencies calculated for the DCNP molecule in vacuum and the data measured for the crystal are in good agreement. The low-frequency vibrations observed in experiment are not seen for isolated molecules because they are associated with the crystal lattice vibrations. Many frequencies associated with vibrations of the molecule skeleton correspond to the proper empirical

DOI: 10.1021/jp510102q
J. Phys. Chem. A 2015, 119, 1347−1358

Table 3. Frequencies of Raman Shift Measured for Single Crystal of DCNP at 295 K and Calculated by HF/6-311G Methodology for Isolated (in Vacuum) DCNP Molecules as Well as Located in Different Solvents

Raman spectrum in crystal	vacuum	acetonitrile	cyclohexane	methanol	tetrahydrofuran	toluene	
397.8		394.5		392.4	372.8	365.9	
417.7		414.7	405.1		411.8	406.8	
451.0		458.2	428.2			429.9	
471.7				480.1			
514.4		515.3		529.1	502.9		
616.7		604.9	599.8		599.9	595.7	
		644.2	642.7	639.5			
666.1		672.9		673.1	655.9	660.7	
693.0	686.9	701.1	699.3		695.2	690.8	pyrazole in-plane
725.3		729.9		718.3	729.3	720.8	phenyl CH out of plane
761.0	754.4	769.7		779.9	781.0		pyrazole in-plane
825.0	808.6		837.2		838.2	839.2	
866.0		878.6	865.5	889.9		862.4	pyrazole stretching
		902.7	903.3		900.9	892.8	
		922.8		924.3	934.2	939.3	
				950.8	955.3		
990.8	1011.2		988.8	984.3	994.4	987.8	
	1038.5	1035.3		1030.5	1038.6		
					1048.9		
		1056.2			1068.4	1058.4	
	1065.4	1088.3	1064.5	1098.3	1097.5		
1158.0	1110.8	1108.4			1159.0	1159.3	
		1132.2					
1184.7	1169.9	1164.2					NN stretching
1228.4	1214.8	1218.3		1201.1	1236.2		CC stretching/CH_2 bending
1296.0	1250.0	1254.3	1241.3	1261.7	1283.2	1277.8	CH bending
		1277.9	1295.2				
1323.4	1349.5	1342.3	1319.5	1337.2	1331.6	1348.1	CH_2 bending
	1389.1		1384.3				
	1403.1		1408.0	1402.7	1414.2	1398.9	
	1448.8	1432.2	1432.3	1425.6	1449.3		
		1491.2	1485.0	1470.8		1485.7	
1504.6	1520.1	1526.1		1546.2			phenyl CH bending
1569.5	1561.9			1565.1		1574.6	pyrazole CN stretching
1598.7	1588.8		1603.2		1592.5		CC stretching
		1663.1	1675.4				
	1674.1	1681.0	1687.3		1675.3	1681.6	
				1758.3			
	1701.1	1787.2	1787.3	1774.7		1787.4	
2221.0	2345.3		2180.7			2127.8	CN stretching

values. The data presented here can be confirmed by the results obtained for fluorescence of the DCNP. The fluorescence spectra of the DCNP crystal phase show a vibrational structure principally similar to the internal vibrational modes of the monomers in an alkane matrix.[39] It is in agreement with the work of Philpott[40] and confirms the not so important interaction between the DCNP structure and surrounding molecules.

The band located around 2345.3 cm^{-1} can be related to the antisymmetric stretching vibration of the two C≡N bonds. The mentioned vibration investigated experimentally for the DCNP molecular crystal shows a peak at 2221 cm^{-1}.[39] In accordance with the work of Taylor and Kennard,[41] the vibration of the C≡N bond shifted to lower wavenumber indicates a significant transfer of electric charge between molecules. The shift of vibrational frequency observed for the DCNP single crystal compared to the frequencies calculated for isolated molecule testifies the existence of the intermolecular charge transfer. In this case, one may conclude that the charge transfer appearing between the DCNP molecules plays the crucial role when the electronic properties of the molecular crystal are investigated.

3.3. UV and Visible Light Absorption Spectra. The electron absorption spectra of the DCNP molecule were calculated using four different methodologies. The time-dependent HF and time-dependent DFT method with B3LYP, LC-BLYP, and CAM-B3LYP potentials were used. The UV−vis spectra calculated for the isolated molecule are presented in Figure 3. One can see that the spectra calculated by DFT methods are red-shifted in comparison to the one computed by the HF method. The first absorption peak calculated for the isolated DCNP molecule is located at 337, 444, 392, and 404 nm, applying HF, B3LYP, LC-BLYP, and CAM-B3LYP methodologies, respectively. The obtained results are in agreement with the usual tendency of used methods. The intensity of the first absorption peak is the highest for all

DOI: 10.1021/jp510102q
J. Phys. Chem. A 2015, 119, 1347−1358

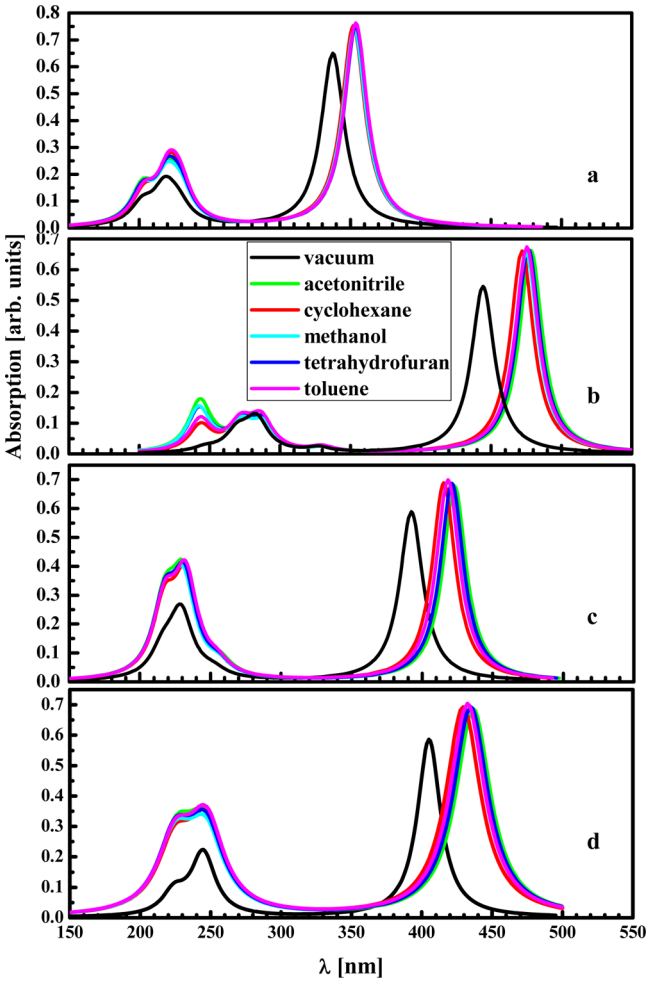

Figure 3. UV−vis spectra calculated for DCNP molecule using the (a) HF/6-311++G** methodology, (b) B3LYP/6-311++G** methodology, (c) LC-BLYP/6-311++G** methodology, and (d) CAM-B3LYP/6-311++G** methodology.

applied quantum-chemical methodologies. In all cases, it is associated with the $\pi \rightarrow \pi^*$ electron transition from the highest occupied molecular orbital (HOMO) to the lowest unoccupied molecular orbital (LUMO). The HOMO and LUMO orbitals calculated by the DFT/B3LYP method are presented as examples in Figure 4. The HOMO is delocalized on the whole molecule, with a significant contribution from the π orbitals of the phenyl ring possessing a donor character. At the same time, only a small decrease of the donor group in the LUMO orbital is observed with a parallel increase of the acceptor contribution. The LUMO is mostly associated with the electronic levels formed by the dicyano group, which possesses acceptor behavior. In this case, the lowest electron transition has a partial intramolecular charge transfer character.

The absorption peaks calculated by the HF method, located between 200−220 nm (see Figure 3a) are associated with the transition from HOMO−2 and HOMO−3 to the LUMO orbital. The UV−vis spectrum calculated with the B3LYP potential is more detailed (Figure 3b). Here the short wavelength peaks are associated with the HOMO-*n*−LUMO electron transfer, but the next peaks are associated with the transition HOMO−LUMO+*n*. The same electron transfer behavior is noticed for the spectrum calculated in a vacuum using LC-BLYP and CAM-B3LYP potentials, but the spectra are less detailed (Figure 3, panels c and d, respectively). The mentioned spectra are something between the one calculated by the HF methodology and the one computed using the B3LYP potential. In conclusion, one may say that the UV−vis spectra calculated by LC-BLYP and CAM-B3LYP are very similar.

The discussion of charge transfer during the excitation process for the transition S_0-S_1 can be analyzed using the approach described in the works of Guido et al.[42] and García et al.[43] The charge transfer parameters were calculated for all HF, B3LYP, LC-BLYP, and CAM-B3LYP methods. Their values are consistent with evaluation of the dipole moment changes specified in Table 1. The values of the charge transfer parameters collected in Table 4 were calculated by the DFT/B3LYP method. The mentioned parameter calculated for the DCNP molecule in vacuum is equal to 0.053420. It is seen that the solvent environment supports the charge transfer mechanism, but because the charge transfer parameters have not so high values, this is not the main mechanism responsible for the optical properties of the molecule.

Table 4. Charge Transfer Parameters and the Positions of First Absorption Peak λ_{max} Calculated by DFT/B3LYP Potential for the DCNP Molecule in Different Solvents and the Experimentally Obtained Data

		λ_{max} (nm)	
solvent	f_{CT}	DFT/B3LYP	exp
cyclohexane	0.068256	471.80	449.59
methanol	0.070243	474.80	461.55
toluene	0.068591	475.22	464.54
tetrahydrofuran	0.069939	476.35	461.70
acetonitrile	0.065623	478.07	462.12

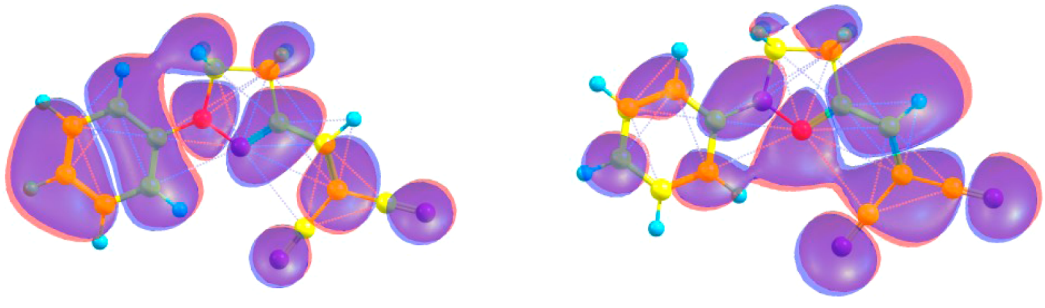

Figure 4. HOMO (left) and LUMO (right) orbitals of DCNP molecule calculated by B3LYP/6-311++G** methodology.

DOI: 10.1021/jp510102q
J. Phys. Chem. A 2015, 119, 1347−1358

The amount of details observed in the calculated UV−vis spectra may be caused by excluding the electron−phonon interaction occurring in the system. The mentioned phenomenon broadens the spectral lines especially at room temperature, but the performed calculations present the state at the temperature of 0 K.

3.4. Effect of Solvent on the Structural and Optical Properties of DCNP. The effect of solvent on the Raman and IR as well on the UV−vis absorption spectra of the DCNP molecule was also investigated. In Table 3 (columns 3−7), the Raman frequencies calculated at the HF/6-311G level in solvents such as acetonitrile, cyclohexane, methanol, tetrahydrofuran, and toluene are collected. The chosen solvents possess different polarity. The values of dielectric constants at zero frequency and infinite ones for all used solvents are presented in Table 1.

The geometry of the DCNP in mentioned solvents were optimized taking into account an equilibrium solute−solvent effect giving the most pronounced interaction with acetonitrile and methanol because these solvents possess the highest ε values. Analyzing the results presented in Table 3 and Figure 5,

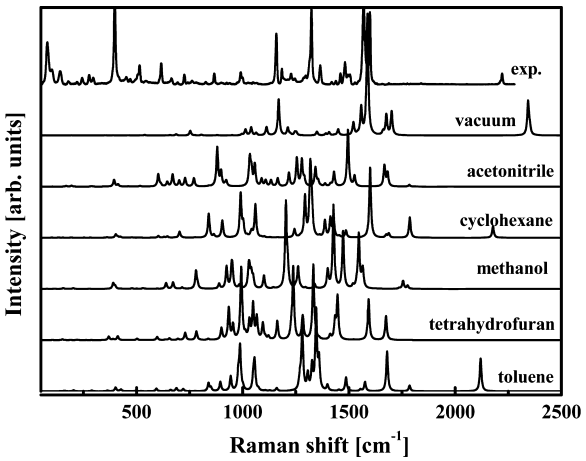

Figure 5. Raman spectra calculated for the DCNP molecule in vacuum and in several solvents calculated by the HF/6-311++G** methodology and compared to experimental data.

one may see that positions of the Raman shift peaks obtained for DCNP in cyclohexane, tetrahydrofuran, and toluene fit with the results obtained for the isolated molecule. These spectra fit also with the experimental results in the range of the molecular skeleton vibrations. It means that in the crystalline phase the system is not characterized by strong hydrogen bonds. It also supports the reason to use the polarizable continuum model to simulate the vibrational frequencies of the DCNP molecule.[44] Solvents as acetonitrile and methanol generally shift the Raman spectra in a direction of higher wavenumbers. From Table 3 as well as from Figures 5 and 6, one can see that there are no imaginary frequencies in the vibrational spectrum of DCNP, indicating its stable configuration in the chosen environment.

The influence of solvent on the vibrational frequencies of organic molecules was investigated theoretically in several works using the PCM model which gives appropriate results.[45−49] We cannot compare our IR data to experimental ones because these measurements were not yet done, and to our knowledge, these properties were not investigated at all. In this case, we will focus on comparing the solvent affected IR spectra to that calculated in vacuum. In analyzing the IR spectra

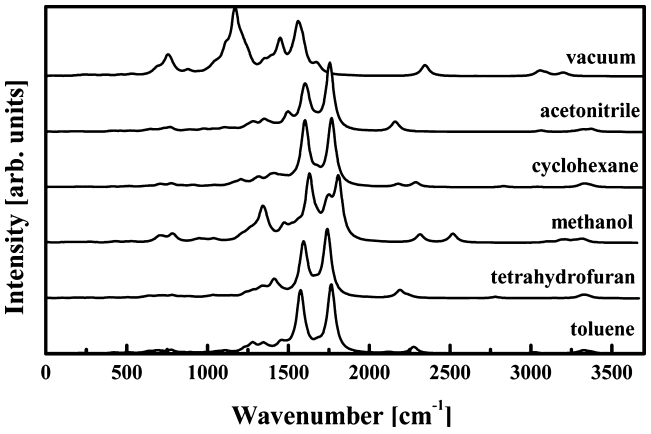

Figure 6. IR spectra calculated for the DCNP molecule in vacuum and in several solvents calculated by the HF/6-311++G** methodology.

calculated for the DCNP molecule in different solvents (see Figure 6), one may see that the solvent-induced alteration of the bonding electron density between the atoms leads to an increase of the vibrational energy relative to that simulated in the gas phase. It is seen that the IR spectrum of an organic compound is not only dependent on its intermolecular bond strength but also strongly affected by the environmental factors such as solvent effect. One may see that all solvent-dependent IR spectra of the DCNP molecule are very similar and should be rescaled by the factor 0.88. In this case, one may see that the vibrations connected to the CC stretching/CH_2 bending modes in the solvent will lose their intensities.

The time-dependent solvation effects can be described in the PCM framework by introducing a time dependence in the apparent surface charges.[50,51] When the light absorption process is studied, it is necessary to take into account the nonequilibrium solute−solvent effect. Analyzing the UV−vis absorption spectra computed by different HF and DFT methods (see Figure 3) for the DCNP molecule, one may conclude that the inclusion of solvent effect shifts all the transitions to lower energy. It is also seen that the polarity of molecule is important because the S_0-S_1 transition depends on the solvent electrostatic properties. Comparing the theoretically obtained results (see Figure 3) with the experimental ones (Figure 7), one may say that the B3LYP methodology is the best in reflecting the empirical data. The spectra presented in Figure 3 were calculated taking into account the vertical electron transitions, but the vibronic influence on the optical properties of DCNP were also studied. Consequently, the equilibrium structure of the DCNP molecule at its first excited state was calculated. The structures of the DCNP optimized at the ground and first excited state are very similar, and absorption of photon induces only minor structural changes because of the rigid backbone of the molecule. It means that the most stable shape of DCNP is characterized by an almost planar rearrangement. The molecule in the first excited state forms the structure presenting geometry features very similar to that of the ground state. The H-bond distances decrease when the dye molecules are in their first excited state. It is in accordance with the work of Pedone et al.[52] The optimization was performed in the solvent environment using HF/6-311G methodology. Then the normal modes of the vibrational frequencies in harmonic approximation were calculated for all structures. The Franck−Condon factor was estimated using the methodology implemented by Barone and co-workers.[53] As a

DOI: 10.1021/jp510102q
J. Phys. Chem. A 2015, 119, 1347−1358

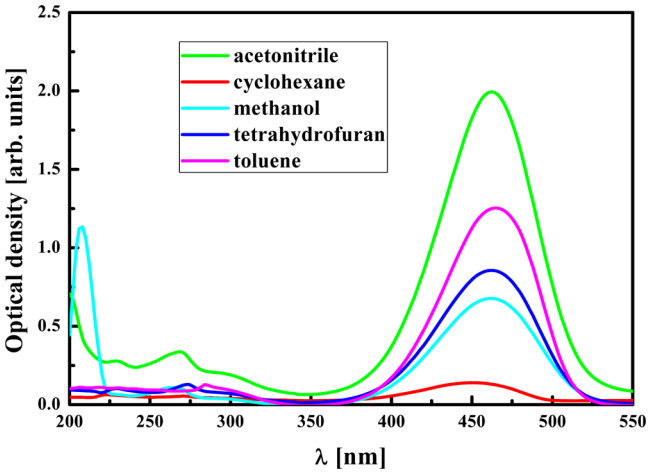

Figure 7. Experimental UV−vis absorption spectra measured for the DCNP molecule dissolved in various solvents.

consequence, UV−vis absorption spectra corresponding to transitions between equilibrated ground electronic state and vertical electronically excited states were calculated.

The obtained results do not show any significant changes in the position of the first absorption peak (λ_{max}). Probably it is due to the low polarity of used solvents and a small number of normal modes calculated for the studied molecule. From the other side, inclusion of the Franck−Condon factor has an important influence on the spectra of the large molecules[54,55] in contrast to the studied DCNP. The calculated spectra including vibronic interaction are broadened in comparison with the spectra with vertical transitions only. Probably the results may change when using the more elaborated methods to compute the Franck−Condon factor,[56] but it will be the aim of future work.

The positions of the first absorption peak λ_{max} obtained theoretically for the DCNP molecule applying the DFT/B3LYP potential, taking into consideration different solvents as well as data defined experimentally are presented in Table 4. Analyzing the experimental data, one can note that the solvatochromic effect is the largest for toluene and acetonitrile then weaker for tetrahydrofuran and methanol, and the less important changes were detected for cyclohexane. Almost the same behavior is obtained applying the DFT/B3LYP procedure to compute UV−vis spectra in proposed solvents (see Table 4 and Figure 3b). The experimentally obtained trend is maintained with one difference that the effect derived from toluene is underestimated by the C-PCM/B3LYP/6-311++G** model. The intermolecular interactions occurring between DCNP and toluene are stronger than those calculated theoretically using the C-PCM model. Probably more elaborate implementation of the PCM model should be used to describe more rigorously the solvent polarization during excitation. As an example, two methodologies such as SS-PCM[57] and corrected LC-PCM[58] may be mentioned. The SS-PCM approach is expected to be more accurate in polar solvents, where the effect of the variation of the dipole moment associated with the electronic transition should be significant.[57] In our case, the transition dipole moment of the DCNP concerning the S_0-S_1 excitation is important, but the toluene is not a polar solvent. Also, the discrete local field model[59] implemented by our group may be applied but it is very time-consuming and makes sense when used in the analysis of nonlinear optical properties of tested materials.[60−62] The mentioned model is very sensitive to the intramolecular electron transfer and may describe the polar character of solute, but the molecular dynamics simulations are needed and the obtained results will probably not be so spectacular.

Moreover, intensity of absorption peaks calculated theoretically cannot be compared to the experimental data because the used methodologies do not take into account the degenerated states. The tendency of solvatochromic changes is maintained for the HF methodology, but the spectra are unnaturally shifted toward the blue side. The effect of solvent on the UV−vis spectrum of DCNP is also not reproduced correctly when applying the LC-BLYP as well as CAM-B3LYP methodology. In this case, the polarity of a solvent is not compatible with the observed solvatochromic effect (experimental data from Table 4). In conclusion, one may say that the HF/6-311++G** and B3LYP/6-311++G** methodologies may be used to reproduce the structural and electronic properties, respectively, of the DCNP molecule qualitatively. Additionally, the compatibility of the B3LYP/6-311++G** calculated results with the experimental data is satisfactory from the quantitative point-of-view. For example, the maximum absorption wavelength of the first π band, calculated by B3LYP/6-311++G** for the DCNP molecule dissolved in tetrahydrofuran, is located at 476.35 nm (see Figure 3b and Table 4), and the measured value is equal to 459.2 nm.[63] It shows a good agreement between theoretical results and experimental data.

As it was performed for the DCNP molecule in the vacuum also in the presence of solvent, the charge transfer parameter f_{CT} was calculated. The data are collected in Table 4, and they confirm that the studied molecule is not characterized by the strong intramolecular charge transfer effect. The charge transfer parameters were calculated for all HF, B3LYP, LC-BLYP, and CAM-B3LYP methods. Their values are consistent with evaluation of the dipole moment changes specified in Table 1. The values of the charge transfer parameters collected in Table 4 were calculated by the DFT/B3LYP method. Comparing these data to the charge transfer parameter calculated for the DCNP molecule in vacuum, which is equal to 0.053420, one can say that the solvent environment supports the charge transfer mechanism but the molecule already shows a partial charge transfer and the observed effect is not so strong.

3.5. Ground State Dipole Moment. It is expected that the large ground state dipole moment of the partially charged transfer molecule depends on the solvent polarity, as is usually the case. To check this dependence, the dipole moment of DCNP was calculated in polar solvents. The solvatochromic effect calculated by the HF method was not so clearly seen as it was noticed for DFT/B3LYP, DFT/LC-BLYP, as well as for DFT/CAM-B3LYP; even the relatively high static dipole moment of DCNP was calculated in vacuum. The reaction field model is very sensitive to the intermolecular charge transfer phenomena, and the dipole moment of the molecule should increase significantly in the solvent environment. The dipole moments of solvents affect the molecules, both at the structural and at the physical property levels.

The obtained results are summarized in Table 3, where the static dipole moments of DCNP calculated in vacuum and in selected solvents are presented. The different solvents change the static dipole moments of DCNP from 9 up to 39% as compared to the dipole moment calculated in vacuum. In all cases the static dipole moment of DCNP in solvent is higher than that in gas phase. The same relations were found by

DOI: 10.1021/jp510102q
J. Phys. Chem. A 2015, 119, 1347−1358

Cramer and Truhlar[64] and by Han and co-workers.[65] Han and others proved that the dipole moment of solute increases with solvent polarity. They determined that dipole moment of nucleic acid in aqueous solution increases by more than 40% in comparison to the value calculated in vacuum.[64] The obtained results are in accordance with our previous work.[66] The most impressive are changes calculated by the DFT/B3LYP methodology. It is the reason why the solvatochromic effect calculated by the DFT/B3LYP potential is the most pronounced compared to HF or other long correlated DFT methods. The ground state dipole moments of DCNP calculated by different methods in vacuum were reported as μ_{00} = 4.4 D[8] or as μ_{00} = 7 D.[12,15] The dipole moment of DCNP calculated in the present work is a little bit larger (see Table 1).

3.6. Linear and Nonlinear Optical Properties. The NLO parameters of the DCNP molecule were calculated within all the previously discussed methodologies but only the B3LYP calculated values are presented. The reason for the B3LYP calculated data selection is connected to the linear optical properties estimation with a sufficient correctness. The UV−vis absorption spectra computed by B3LYP/6-311++G** potential give good qualitative results in comparison to the experimentally obtained data. From the other side, the chosen NLO parameters go well with the experimental results. The polarizability, as well as first and second hyperpolarizabilities were calculated for the DCNP molecule in vacuum using the B3LYP/6-311++G** methodology. The investigated molecule was rotated, and its dipole moment was aligned along the *Z* axis (see Figure 8). The calculated values of the static polarizability

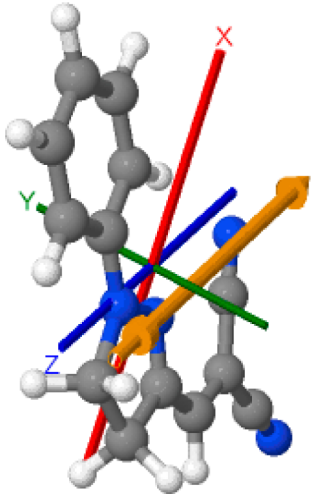

Figure 8. Orientation of DCNP molecule in molecular reference frame and the direction of electric dipole moment μ_z calculated by B3LYP/6-311++G** methodology.

tensor and its average value are presented in Table 5. One may observe that the highest value has the α_{xx} polarizability component. Also, the first-order hyperpolarizability β has the most important value when the output signal is detected in the direction of the *X* axis. The static β_{zzz} has the relatively low value and is negative. These results confirm the information obtained when calculating IR and Raman spectra. It was proved that the DCNP molecule has a static dipole moment mostly created by the charges located at the dicyano and pyrazole group, but the induced charge transfer occurs along the molecule long axis. It is well-known that the first molecular

Table 5. Static ($\lambda = \infty$) Linear Polarizability $\alpha(0)$, First $\beta(0)$, and Second $\gamma(0)$ Hyperpolarizability Tensor Components Obtained for DCNP Molecule in Vacuum Using the B3LYP/6-311++G Methodology in Atomic (au) and Electrostatic (esu) Units[a]**

tensor components	computed values (au)	computed values (esu)
α_{av}	190.58	28.2×10^{-24}
α_{xx}	224.84	33.3×10^{-24}
α_{yy}	131.57	19.5×10^{-24}
α_{zz}	215.33	31.9×10^{-24}
β_{xxz}	1727.23	1.49×10^{-29}
β_{xxx}	1641.32	1.42×10^{-29}
β_{xzz}	1634.98	1.41×10^{-29}
β_{zzz}	−48.21	-0.0042×10^{-29}
β_{z}	4109.68	3.55×10^{-29}
γ_{zzzz}	137738.36	6.94×10^{-35}
γ_{xxxx}	261105.10	13.2×10^{-35}
γ_{xxzz}	148963.36	7.50×10^{-35}
γ_{zzzZ}	137738.36	6.94×10^{-35}

[a]Data calculated in molecular frame coordinate system.

hyperpolarizability β depends not only on the strength of the donor and acceptor groups but also on the nature of the π-conjugated spacer through which they interact. Figure 8 shows that the DCNP molecule is characterized predominantly by aromatic ground states, and according to the work of Andreu et al.,[67] this kind of D-π−*A* system should favor the intramolecular charge transfer process. The molecular hyperpolarizability of DCNP along the charge transfer direction is equal to $\beta_0 = 44.7 \times 10^{-30}$ esu at zero energy.[8] The value of static β_z presented in Table 5 ($\beta_z = 35.5 \times 10^{-30}$ esu) is in good agreement with the experimentally obtained value. The difference is due to the fact that the hyperpolarizability presented here was calculated for an isolated molecule and the order of the DCNP molecules in the molecular crystal may increase the output signal. It was seen from the calculations of vibrational modes that in the DCNP molecular crystal intermolecular charge transfer is observed. The highest value of static second order hyperpolarizability is also noticed for the γ_{xxxx} component, proving the above presented conclusions. In Table 6 are presented the dominant

Table 6. First SHG [$\beta(-2\omega;\omega,\omega)$] and Second OKE [$\gamma(-\omega;\omega,\omega,-\omega)$] Hyperpolarizabilities Calculated at λ = 1064 nm Fundamental Wavelength for DCNP Molecule in Vacuum Using B3LYP/6-311++G Methodology in Atomic (au) and Electrostatic (esu) Units[a]**

tensor components	computed values (au)	computed values (esu)
$\beta_{zxx}(-2\omega;\omega,\omega)$	−543948.84	-47.0×10^{-28}
$\beta_{zxz}(-2\omega;\omega,\omega)$	−388854.31	-33.6×10^{-28}
$\beta_{zzz}(-2\omega;\omega,\omega)$	−360316.13	-31.3×10^{-28}
$\beta_{xxx}(-2\omega;\omega,\omega)$	379677.15	32.8×10^{-28}
$\beta_{z}(-2\omega;\omega,\omega)$	−1088846.91	-94.1×10^{-28}
$\beta_{x}(-2\omega;\omega,\omega)$	930156.17	80.4×10^{-28}
$\gamma_{xxxx}(-\omega;\omega,\omega,-\omega)$	35885925.18	1807.6×10^{-35}
$\gamma_{zxxz}(-\omega;\omega,\omega,-\omega)$	26956468.10	1357.8×10^{-35}
$\gamma_{zzxx}(-\omega;\omega,\omega,-\omega)$	23827427.16	1200.2×10^{-35}
$\gamma_{xzzx}(-\omega;\omega,\omega,-\omega)$	22479695.58	1132.3×10^{-35}
$\gamma_{xxzz}(-\omega;\omega,\omega,-\omega)$	21800381.93	1098.1×10^{-35}
$\gamma_{zzzz}(-\omega;\omega,\omega,-\omega)$	21433642.36	1079.6×10^{-35}

[a]Data calculated in molecular frame coordinate system.

DOI: 10.1021/jp510102q
J. Phys. Chem. A 2015, 119, 1347−1358

components of the frequency-dependent first and second hyperpolarizabilities calculated for the second harmonic generation (SHG) phenomena and two photon absorption (TPA) occurrence, respectively, $\lambda = 2\pi c/\omega = 1064$ nm. The highest value of frequency-dependent first-order hyperpolarizability is observed for component $\beta_{zxx}(-2\omega;\omega,\omega)$, and of the second order, hyperpolarizability is observed for the $\gamma_{xxxx}(-\omega;\omega,\omega,-\omega)$ component. It is seen that for the frequency-dependent first-order hyperpolarizability, the induced dipole moment takes contribution from the static one, and the z component of β appears here.

3. 7. SHG Susceptibility–Comparison with Experiment. To make comparison of the computed and experimental values of quadratic NLO properties, it is important to express the first ones in the laboratory reference frame, in which the NLO susceptibility was measured. On the molecular level, the NLO response is related to the change of the molecule dipole moment μ induced by the action of the applied, external electric field, whose ith component is given by

$$\Delta\mu_i = \mu_i(E) - \mu_i(0) = W \sum_j \sum_k \beta_{ijk} E_j E_k \tag{1}$$

where the E's is an electric field experienced by a molecule. The factor W depends on the convention used for the definition of the Fourier transform of electric field and taking into account or not the degeneration factors (see, for example, Rau et al.[68]).

For noninteracting molecules arranged in a single crystal, the macroscopic, interesting for practical applications, and for binary-composite materials the (I,J,K) component of the second-order NLO susceptibility tensor $\chi^{(2)}_{IJK}(-2\omega;\omega,\omega)$, describing the SHG process, can be obtained by transformation of corresponding quantities from the molecular to the macroscopic reference frame with what is given using the following equation:

$$\chi^{(2)}_{IJK}(-2\omega;\omega,\omega) = N^s F^s \sum_i \sum_j \sum_k a^s_{Ii} a^s_{Jj} a^s_{Kk} \beta^s_{ijk}(-2\omega;\omega,\omega) + N^m F^m \sum_i \sum_j \sum_k a^m_{Ii} a^m_{Jj} a^m_{Kk} \beta^m_{ijk}(-2\omega;\omega,\omega) \tag{2}$$

where (i,j,k) and (I,J,K) subscripts refer to molecular and laboratory reference frames, superscipts s and m refer to guest and host molecules, respectively, a_{Ij} are Wigner rotation matrix elements, $N^{s(m)}$ are densities of guest (s) and host (m) molecules, and $F^{s(m)}$ are the corresponding local field factors. Usually the Lorentz–Lorenz formula is taken into account:

$$F^{s(m)} = (f^{s(m)}_{\omega})^2 f^{s(m)}_{2\omega} = \left[\frac{n^2_{\omega}+2}{3}\right]^2 \frac{n^2_{2\omega}+2}{3} \tag{3}$$

where $n_{\omega(2\omega)}$ are refractive indices at optical frequencies ω and 2ω.

For a host–guest system, polymer/NLO chromophore, the second term in eq 2, can be neglected, as due to centrosymmetric arrangement of polymer chains the polymer second-order susceptibility is null. When these polymers with NLO chromophores are poled at elevated temperature by an application of an intense DC electric field, the NLO chromophores, usually possessing a large ground state dipole moment, orient in its direction, creating noncentrosymmetry in the material. As a consequence, in poled polymers with point symmetry ∞mm, the diagonal component of quadratic susceptibility is given by a configurational average < > over all possible orientations of molecules:

$$\chi^{(2)}_{ZZZ}(-2\omega;\omega,\omega) = N^s F^s < \beta^s_{ijk}(-2\omega;\omega,\omega)\cos^3\Theta >_{ijk} \tag{4}$$

where Z is the poling field direction and Θ is the angle between the applied poling field and the molecule dipole moment. For the charge transfer molecules, the first hyperpolarizability β_{zzz} component is enhanced in the charge transfer direction Z, so the others can be neglected with respect to this one. In that case, eq 4 can be simplified:

$$\chi^{(2)}_{ZZZ}(-2\omega;\omega,\omega) = N^s F^s \beta_{zzz}(-2\omega;\omega,\omega) < \cos^3\Theta > \tag{5}$$

where the average < > describes the amount of polar order.

As already mentioned in Introduction, Manea et al.[9] measured $\chi^{(2)}_{ZZZ}(-2\omega;\omega,\omega)$ susceptibility of a poled PMMA/DCNP guest–host system with a 2 wt % doping level. Taking for DCNP its molecular mass of $M_w = 222.25$ g/mol, one gets for the molecule number density, $N^s = 7.3 \times 10^{19}$ mol/cm^3. Taking for PMMA/DCNP refractive indices $n_{\omega} = 1.4795$ and $n_{2\omega} = 1.5009$ as determined by Swalen et al.[69] for PMMA thin films, one gets for the local field factor the value $F = 2.15$. Furthermore, taking for $<\cos^3\Theta>$ the value of order parameter $<P_2> = 0.3$ as obtained from the optical absorption spectrum variation due to the poling and the charge transfer component $\beta_{zzz} = 3.28 \times 10^{-27}$ esu (Table 5), one gets for the diagonal component $\chi^{(2)}_{ZZZ} = 5.28 \times 10^{-7}$ esu. In SI units, this value is equal to $\chi^{(2)}_{ZZZ}(-2\omega;\omega,\omega) = 64.5$ pm/V, to be compared with the measured one of $\chi^{(2)}_{ZZZ}(-2\omega;\omega,\omega) = 100 \pm 15$ pm/V. Taking account of experimental uncertainties as well as that in the calibration value of quartz, excellent agreement between the computed and the measured values is obtained.

The presented results suggest that the second-order susceptibilities corresponding to the SHG may be calculated for PMMA/DCNP using the simple oriented-gas model and not necessarily the rigorous local field approach.[59] These satisfactory results were obtained maybe because of the low concentration of the DCNP taken into consideration or maybe due to uncorrelated ICT mechanism and the molecule dipole moment direction.

4. CONCLUSIONS

In this paper, we have reported first principle quantum chemical calculations of electronic and vibrational properties performed for the push–pull π electron conjugated DCNP molecule. Its geometry was determined using the HF/6-31G methodology. The molecule was found to be planar with quasi 1D π electron conjugation. A very good agreement between the computed and measured bond lengths was observed what may lead to conclusion that the HF methodology is appropriate to compute the structural properties contrary to the DFT methodology which very often overestimates the bond length.

On the basis of obtained molecule geometry infrared absorption and Raman spectra were computed within the HF/6-311++G** formalism. The obtained spectra give an idea that in the DCNP molecule at the same vibrational modes, its dipole moment and the polarizability change. It impacts the linear optical and mostly the nonlinear optical properties of investigated material because the mentioned phenomena occur

DOI: 10.1021/jp510102q
J. Phys. Chem. A 2015, 119, 1347–1358

when the intramolecular charge transfer mechanism is not dominant.

Four different methodologies: time-dependent HF and time-dependent DFT method with B3LYP, LC-BLYP, and CAM-B3LYP potentials were used to compute the electronic properties of DCNP. The static dipole moment of the investigated molecule calculated by these methods has very similar values being approximately equal to 8 D. This value is in good agreement with the experimental one reported to be equal to 7 D. The observed discrepancy may be due to the intramolecular multipolar interaction which is not taken into account here. The mentioned effect should be crucial here due to the intermolecular charge transfer postulated on the basis of the vibrational properties calculations. Studying the influence of solvent on the IR and Raman spectra, one can conclude that the skeleton of the DCNP is relatively rigid. It gives impact on the S_0-S_1 transition. The discussion of charge transfer during the excitation process for the transition S_0-S_1 was performed. The charge transfer parameters calculated by all chosen methodologies are consistent with evaluation of the dipole moment changes versus solvent effect. The charge transfer parameter f_{CT} calculated by DFT/B3LYP for the DCNP molecule in vacuum is equal to 0.053420. It is seen that the solvent environment weakly enhances the molecular charge transfer.

Also the influence of solvent on electronic structure of DCNP was studied within the PCM model. Dependence of the ground state dipole moment on solvent polarity was also calculated using the four methods mentioned above. In all cases, the dipole moment is larger in the solvent environment than in vacuum, as expected. The change varies from 9% to 39%. Also these methods were used to calculate the influence of solvent on optical absorption spectra (solvatochromic effect). The computed values were compared with available experimental data. Generally, a good agreement was observed for the spectra calculated by the DFT/B3LYP methodology. For example, for the studied molecule, the computed maximum absorption wavelength is of 476.1 nm, whereas the experimental value is of 459.2 nm. The HOMO and LUMO orbitals calculated for DCNP show that the molecular ground state is located at its aromatic part.

The DFT/B3LYP methodology was used to compute the NLO properties of DCNP due to its accuracy in calculation of UV−vis absorption spectra. As it was for linear optical properties, the good agreement is observed also for second-order NLO signal. Estimated from the computation, the diagonal components of $\chi^{(2)}_{ZZZ}(-2\omega;\omega,\omega)$ susceptibility is equal to 64.5 pm/V, whereas the measured one is of 100 ± 15 pm/V. This agreement will be even better if we recalibrate the quartz standard value measured by Manea et al.[9] to the recently introduced one (0.6 pm/V[70] instead of used 1 pm/V[71]). It will give DCNP $\chi^{(2)}_{XXX}(-2\omega;\omega,\omega)$ = 60 ± 9 pm/V, in excellent agreement with the computed one.

The presented results suggest that the second-order susceptibilities corresponding to the SHG may be calculated for PMMA/DCNP using the simple oriented-gas model contrary to the rigorous local field approach. In conclusion, we can say that the used here B3LYP/6-311++G** methodology gives a good description of electronic structure as well as linear and nonlinear optical properties of quasi one-dimensional charge transfer molecules.

The aim of the presented work was to show that for the molecules with not so important internal charge transfer, the macroscopic NLO properties like susceptibility can be calculated by a simple model without the use of complicated local field estimation. In the presented case of specific molecules such as DCNP where the dipole moment direction is not parallel to the charge transfer path, the discrete local field model proposed in our previous work is not necessary to be used.

AUTHOR INFORMATION

Corresponding Author

*E-mail: m.makowska@ajd.czest.pl.

Notes

The authors declare no competing financial interest.

ACKNOWLEDGMENTS

Calculations have been carried out in Wroclaw Center for Networking and Supercomputing (http://www.wcss.wroc.pl) (Grant 171). A.M. acknowledges the support from the Polish National Science Center under project Dec −2011/03/B/ST5/01021. I.R. acknowledges the financial support of Romanian Ministry of Education, Research, Youth and Sports, through the UEFISCDI organism, under Contract no. 279/7.10.2011, Code Project PN-II-ID-PCE-2011-3-05053

REFERENCES

(1) Black, S. N.; Davey, R. J.; Morley, P. R.; Halfpenny, P.; Shepherdb, E. E. A.; Sherwoodb, J. N. Crystal growth and characterisation of the electro-optic material 3-(2,2-Dicyanoethenyl)-1-phenyl-4,5-di hydro-1H-pyrazole. *J. Mater. Chem.* **1993**, *3*, 129−132.

(2) Miniewicz, A.; Palewska, K.; Karpinski, P.; Sznitko, L.; Zielinski. M. Fluorescence and SHG in organic nanocrystals of DCNP. *Proc. SPIE* **2012**, *846400*, 10.1117/12.931663.

(3) Miniewicz, A.; Palewska, K.; Sznitko, L.; Lipiński, J. Single- and two-photon excited fluorescence in organic nonlinear optical single crystal 3-(1,1-Dicyanoethenyl)-1-phenyl-4, 5-dihydro-1H-pyrazole. *J. Phys. Chem. A* **2011**, *115*, 10689−10697.

(4) Sznitko, L.; Myśliwiec, J.; Parafiniuk, K.; Szukalski, A.; Palewska, K.; Bartkiewicz, S.; Miniewicz, A. Amplified spontaneous emission in polymethyl methacrylate doped with 3-(1,1-dicyanoethenyl)-1-phenyl-4,5-dihydro-1H-pyrazole (DCNP). *Chem. Phys. Lett.* **2011**, *512*, 247−250.

(5) Myśliwiec, J.; Sznitko, L.; Szukalski, A.; Parafiniuk, K.; Bartkiewicz, S.; Miniewicz, A.; Sahraoui, B.; Rau, I.; Kajzar, F. Amplified spontaneous emission of 3-(1,1-dicyanoethenyl)-1-phenyl-4,5-dihydro-1H-pyrazole molecule embedded in various polymer matrices. *Opt. Mater.* **2012**, *34*, 1725−1728.

(6) Cole, J. M. Structural studies of organic and organometallic compounds using x-ray and neutron techniques. Ph.D. Thesis, Durham University, 1997.

(7) Allen, S.; McLean, T. D.; Gordon, P. F.; Bothwell, B. D.; Hursthouse, M. B.; Karaulov, S. A. A novel organic electro-optic crystal: 3-(1,1-dicyanoethenyl)-1-phenyl- 4,5-dihydro-1H-pyrazole. *J. Appl. Phys.* **1988**, *64*, 2583−2590.

(8) Miniewicz, A.; Palewska, K.; Lipinski, J.; Kowal, R.; Swedek, B. On the spectroscopic and nonlinear optical properties of 3-(1,1-dicyanoethenyl)-1-phenyl-4,5-dihydro-1H-pyrazole (DCNP). *Mol. Cryst. Liq. Cryst.* **1994**, *253*, 41−50.

(9) Manea, A.-M.; Rau, I.; Tane, A.; Kajzar, F.; Sznitko, L.; Miniewicz, A. Poling kinetics and second order NLO properties of DCNP doped PMMA based thin film. *Opt. Mater.* **2014**, *36*, 69−74.

(10) Kajzar, F.; Jen, A.; Lee, K. S. Polymeric Materials and Their Orientation Techniques for Second-Order Nonlinear Optics. In *Polymers for Photonics Applications II: Nonlinear Optical, Photorefractive and Two-Photon Absorption Polymers*, Lee, K. S., Wegner, G., Eds.; Advances in Polymer Science; Springer-Verlag: Berlin, 2003, Vol. *161*, pp 1−85.

DOI: 10.1021/jp510102q
J. Phys. Chem. A 2015, 119, 1347−1358

(11) Dalton, L. R. Nonlinear Optical Polymeric Materials: From Chromophore Design to Commercial Applications. In *Polymers for Photonics Applications I: Nonlinear Optical and Electroluminescence Polymers*, Lee, K. S., Wegner, G., Eds.; Advances in Polymer Science; Springer-Verlag: Berlin, 2002, Vol. *158*, pp 1−86.
(12) Shi, W.; Fang, C.; Xu, Z.; Pan, Q.; Gu, Q.; Xu, D.; Wei, H.; Yu, J. Poling and characterization of nonlinear polymer DCNP/PEK-c thin films. *Sol. State Commun.* **2000**, *113*, 483−487.
(13) Shi, W.; Fang, C.; Pan, Q.; Sun, X.; Gu, Q.; Xu, D.; Yu, J. Electro-optic properties of poled guest-host organic polymer DCNP/PEK-c thin films. *J. Mater. Sci. Lett.* **2000**, *19*, 147−149.
(14) Marder, S. R.; Cheng, L.-T.; Tiemann, B. G.; Friedli, A. C.; Blanchard-Desce, M.; Perry, J. W.; Skindhoj, J. Large first hyperpolarizabilities in push-pull polyenes by tuning of the bond length alternation and aromaticity. *Science* **1994**, *263*, 511−514.
(15) Shi, W.; Fang, C.-S.; Pan, Q.-W.; Sun, X.; Gu, Q.-T.; Xu, D.; Wei, H.-Z.; Yu, J.-Z. Electro-optical properties and temporal stability of the guest-host DCNP/PEK-c polymer thin film. *Chin. Phys. Lett.* **2000**, *17*, 22−24.
(16) Cole, J. M.; Wilson, C. C.; Howard, J. A. K.; Cruickshank, F. R. Quantitative analysis of hydrogen bonding and atomic thermal motion in the organic non-linear optical material DCNP using X-ray and neutron diffraction. *Acta Cryst. B* **2000**, *56*, 1085−1093.
(17) Schmidt, M. W.; Baldrige, K. K.; Boatz, J. A.; Elbert, S. T.; Gordon, M. S.; Jensen, J. H.; Koseki, S.; Matsunaga, N.; Nguyen, K. A.; Su, S.; et al. General atomic and molecular electronic structure system. *J. Comput. Chem.* **1993**, *14*, 1347−1363.
(18) Gordon, M. S.; Schmidt, M. W. Advances in electronic structure theory: GAMESS a Decade Later. In *Theory and Applications of Computational Chemistry: the first forty years*; Dykstra, C. E., Frenking, G., Kim, K. S., Scuseria, G. E., Eds.; Elsevier: Amsterdam, 2005, pp 1167−1189.
(19) Roothaan, C. C. J. New developments in molecular orbital theory. *Rev. Mod. Phys.* **1951**, *23*, 69−89.
(20) Jensen, F. Locating transition structures by mode following: A comparison of six methods on the Ar8 Lennard-Jones potential. *J. Chem. Phys.* **1995**, *102*, 6706−6718.
(21) Becke, A. D. Density-functional exchange-energy approximation with correct asymptotic behavior. *Phys. Rev. A* **1988**, *38*, 3098−3100.
(22) Becke, A. D. Density-functional thermochemistry. III. The role of exact exchange. *J. Chem. Phys.* **1993**, *98*, 5648−5652.
(23) Lee, C.; Yang, W.; Parr, R. G. Development of the colic-salvetti correlation-energy formula into a functional of the electron density. *Phys. Rev. B* **1988**, *37*, 785−789.
(24) Iikura, H.; Tsuneda, T.; Yanai, T.; Hirao, K. A long-range correction scheme for generalized-gradient-approximation exchange functionals. *J. Chem. Phys.* **2001**, *115*, 3540−3544.
(25) Yanai, T.; Tew, D. P.; Handy, N. C. A new hybrid exchange-correlation functional using the coulomb-attenuating method (CAM-B3LYP). *Chem. Phys. Lett.* **2004**, *393*, 51−57.
(26) Haharan, P. C.; Pople, J. A. The influence of polarization functions on molecular orbital hydrogenation energies. *Theoret. Chim. Acta* **1973**, *28*, 213−222.
(27) Frisch, M. J.; Pople, J. A.; Binkley, J. S. Self-consistent molecular orbital methods 25. Supplementary functions for Gaussian basis sets. *J. Chem. Phys.* **1984**, *80*, 3265−3269.
(28) Clark, T.; Chandrasekhar, J.; Spitznagel, G. W.; Schleyer, P. Efficient diffuse function-augmented basis sets for anion calculations. III. The 3-21+G set for first-row elements, Li-F. *J. Comput. Chem.* **1983**, *4*, 294−301.
(29) Davidson, E. R. The iterative calculation of a few of the lowest eigenvalues and corresponding eigenvectors of large real-symmetric matrices. *J. Comput. Phys.* **1975**, *17*, 87−94.
(30) Miertus, S.; Scrocco, E.; Tomasi, J. Electrostatic interaction of a solute with a continuum. A direct utilization of *ab initio* molecular potentials for the prevision of solvent effects. *Chem. Phys.* **1981**, *55*, 117−129.
(31) Barone, V.; Cossi, M. Quantum calculation of molecular energies and energy gradients in solution by a conductor solvent model. *J. Phys. Chem. A* **1998**, *102*, 1995−2001.
(32) Cossi, M.; Rega, N.; Scalmani, G.; Barone, V. Energies, structures, and electronic properties of molecules in solution with the C-PCM solvation model. *J. Comput. Chem.* **2003**, *24*, 669−681.
(33) Tomasi, J.; Mennucci, B.; Cammi, R. Quantum mechanical continuum solvation models. *Chem. Rev.* **2005**, *105*, 2999−3093.
(34) Cossi, M.; Mennucci, B.; Cammi, R. Analytical first derivatives of molecular surfaces with respect to nu clear coordinates. *J. Comput. Chem.* **1996**, *17*, 57−73.
(35) Carlier, P. R.; Deora, N.; Crawford, T. D. Protonated 2-methyl-1,2-epoxypropane: A challenging problem for density functional theory. *J. Org. Chem.* **2006**, *71*, 1592−1597.
(36) Jensen, K. P.; Roos, B. O.; Ryde, U. Performance of density functionals for first row transition metal systems. *J. Chem. Phys.* **2007**, *126*, 014103−014114.
(37) Scott, A. P.; Radom, L. Harmonic vibrational frequencies: An evaluation of Hartree−Fock, Møller−Plesset, quadratic configuration interaction, Density Functional Theory, and semiempirical scale factors. *J. Phys. Chem.* **1996**, *100*, 16502−16513.
(38) Ruiz Delgado, M. C.; Hernandez, V.; Casado, J.; Lopez Navarrete, J. T.; Raimundo, J. M.; Blanchard, P.; Roncali, J. Vibrational study of push−pull chromophores for second-order non-linear optics derived from rigidified thiophene π-conjugating spacers. *J. Mol. Struct.* **2003**, *651−653*, 151−158.
(39) Morawski, O.; Sobolewski, A. L.; Kozankiewicz, B.; Sznitko, L.; Miniewicz, A. On the origin of fluorescence emission in optically non-linear DCNP crystals. *Phys. Chem. Chem. Phys.* **2014**, *16*, 26887−26892.
(40) Philpott, M. R. Theory of the coupling of electronic and vibrational excitations in molecular crystals and helical polymers. *J. Chem. Phys.* **1971**, *55*, 2039−2054.
(41) Taylor, R.; Kennard, O. Crystallographic evidence for the existence of C−H···O, C−H···N and C−H···Cl hydrogen bonds. *J. Am. Chem. Soc.* **1982**, *104*, 5063−5070.
(42) Guido, C. A.; Mennucci, B.; Jacquemin, D.; Adamo, C. Planar vs. twisted intramolecular charge transfer mechanism in Nile Red: New hints from theory. *Phys. Chem. Chem. Phys.* **2010**, *12*, 8016−8023.
(43) García, G.; Adamo, C.; Ciofini, I. Evaluating push−pull dye efficiency using TD-DFT and charge transfer indices. *Phys. Chem. Chem. Phys.* **2013**, *15*, 20210−20219.
(44) Stefanovich, E. V.; Truong, T. N. An *ab initio* study of solvent shifts in vibrational spectra. *J. Chem. Phys.* **1996**, *105*, 2961−2871.
(45) Glover, W. J.; Larsen, R. E.; Schwartz, B. J. How does a solvent affect chemical bonds? Mixed quantum/classical simulations with a full CI treatment of the bonding electrons. *J. Phys. Chem. Lett.* **2010**, *1*, 165−169.
(46) Li, Y.; Jiang, L. Solvent effect on characteristic vibration of IR spectrum of 4,4′-Dibromodiphenyl ether] giving suitable results. *Chem. Res. Chin. Univ.* **2014**, *30*, 997−1004.
(47) Babu, N. S.; Lelisho, T. A. Computational studies of solvent effects on structure and vibrational spectra of isofavonoid 5,7-Dihydroxy-3-(4-hydroxyphenyl)chromen-4-one(Genistein) by ab intio HF and DFT methods. *Adv. Appl. Sci. Res.* **2012**, *3*, 3916−3934.
(48) Nandini, G.; Sathyanarayana, D. N. Ab initio studies of solvent effect on molecular conformation and vibrational spectra of diacetamide. *Spectrochim. Acta, Part A* **2004**, *60*, 1115−1126.
(49) Sowula, M.; Misiaszek, T.; Bartkowiak, W. Solvent effect on the vibrational spectrum of Michler's ketone. Experimental and theoretical investigations. *Spectrochim. Acta, Part A* **2014**, *131*, 678−685.
(50) Caricato, M.; Ingrosso, F.; Mennucci, B.; Tomasi, J. A time-dependent polarizable continuum model: Theory and application. *J. Chem. Phys.* **2005**, *122*, 154501.
(51) Caricato, M.; Mennucci, B.; Tomasi, J.; Ingrosso, F.; Cammi, R.; Corni, S.; Scalmani, G. Formation and relaxation of excited states in solution: a new time dependent polarizable continuum model based on time dependent density functional theory. *J. Chem. Phys.* **2006**, *124*, 124520.

DOI: 10.1021/jp510102q
J. Phys. Chem. A 2015, 119, 1347−1358

(52) Pedone, A.; Bloino, J.; Barone, V. Role of host-guest interactions in tuning the optical properties of coumarin derivatives incorporated in MCM-41: A TD-DFT investigation. *J. Phys. Chem. C* **2012**, *116*, 17807−17818.
(53) Improta, R.; Barone, V.; Santoro, F. Ab initio calculations of absorption spectra of large molecules in solution: Coumarin C153. *Angew. Chem., Int. Ed.* **2007**, *46*, 405−408.
(54) Santoro, F.; Improta, R.; Lami, A.; Bloino, J.; Barone, V. Effective method to compute Franck-Condon integrals for optical spectra of large molecules in solution. *J. Chem. Phys.* **2007**, *126*, 084509−084513.
(55) Santoro, F.; Improta, R.; Lami, A.; Bloino, J.; Barone, V. Erratum: "Effective method to compute Franck-Condon integrals for optical spectra of large molecules in solution. *J. Chem. Phys.* **2007**, *126*, 169903−169911.
(56) Bloino, J.; Biczysko, M.; Santoro, F.; Barone, V. General approach to compute vibrationally resolved one-photon electronic spectra. *J. Chem. Theory Comput.* **2010**, *6*, 1256−1274.
(57) Improta, R.; Barone, V.; Scalmani, G.; Frisch, M. J. A state-specific polarizable continuum model time dependent density functional theory method for excited state calculations in solution. *J. Chem. Phys.* **2006**, *125*, 054103−054109.
(58) Caricato, M.; Mennucci, B.; Tomasi, J.; Ingrosso, F.; Cammi, R.; Corni, S.; Scalmani, G. Formation and relaxation of excited states in solution: A new time dependent polarizable continuum model based on time dependent density functional theory. *J. Chem. Phys.* **2006**, *124*, 124520-1−124520-13.
(59) Reis, H.; Makowska-Janusik, M.; Papadopoulos, M. G. Nonlinear optical susceptibilities of poled guest-host systems: A computational approach. *J. Phys. Chem. B* **2004**, *108*, 8931−8940.
(60) Makowska-Janusik, M.; Kassiba, A.; Failleau, G.; Bouclé, J. Interface effects on the NLO properties of guest-host materials. *Mater. Sci.* **2006**, *24*, 891−900.
(61) Makowska-Janusik, M. Influence of the polymeric matrix on the NLO molecular response in guest-host materials. *Nonlinear Opt., Quantum Opt.* **2007**, *37*, 75−85.
(62) Makowska-Janusik, M. Optical Properties and Structural Rearrangement of Guest NLO Molecules Studied by Different Solvation Models. *Nonlinear Opt., Quantum Opt.* **2012**, *45*, 41−51.
(63) Miniewicz, A.; Delysse, S.; Nunzi, J. M.; Kajzar, F. Two-photon absorption resonance in 3-1,1-dicyanoethenyl-1-phenyl-4,5-dihydro-1H-pyrazole (DCNP). *Chem. Phys. Lett.* **1998**, *287*, 17−21.
(64) Cramer, C. J.; Truhlar, D. G. Implicit solvation models: Equilibria, structure, spectra, and dynamics. *Chem. Rev.* **1999**, *99*, 2161−2200.
(65) Han, W.-G.; Liu, T.; Himo, F.; Toutchkine, A.; Bashford, D.; Hahn, K. M.; Noodleman, L. A Theoretical Study of the UV/Visible absorption and emission solvatochromic properties of solvent sensitive dyes. *ChempPhysChem* **2003**, *4*, 1084−1094.
(66) Makowska-Janusik, M.; Kityk, I. V.; Kulhanek, J.; Bures, F. Peculiarities of the environmental influence on the optical properties of push-pull nonlinear optical molecules: A theoretical study. *J. Phys. Chem. A* **2011**, *115*, 12251−12258.
(67) Andreu, R.; Jesus Blesa, M.; Carrasquer, L.; Garın, J.; Orduna, J.; Villacampa, B.; Alcala, R.; Casado, J.; Ruiz Delgado, M. C.; Navarrete, J. T. L.; Allain, M. Tuning first molecular hyperpolarizabilities through the use of proaromatic spacers. *J. Am. Chem. Soc.* **2005**, *127*, 8835−8845.
(68) Rau, I.; Kajzar, F.; Luc, J.; Sahraoui, B.; Boudebs, G. Comparison of Z-scan and THG derived nonlinear index of refraction in selected organic solvents. *J. Opt. Soc. Am. B* **2008**, *25*, 1738−1747.
(69) Swalen, J. D.; Rieckoff, K. E.; Tacke, M. Optical properties of arachidate monolayers by integrated optical techniques. *Opt. Commun.* **1978**, *24*, 146−148.
(70) Boyd, R. W. *Nonlinear Optics*, 3rd ed.; Academic Press: London, 2008; p 50.
(71) Choy, M. M.; Byer, R. L. Accurate second-order susceptibility measurements of visible and infrared nonlinear crystals. *Phys. Rev. B* **1976**, *14*, 1693−1706.

DOI: 10.1021/jp510102q
J. Phys. Chem. A 2015, 119, 1347−1358